

# RSC Advances



This is an *Accepted Manuscript*, which has been through the Royal Society of Chemistry peer review process and has been accepted for publication.

*Accepted Manuscripts* are published online shortly after acceptance, before technical editing, formatting and proof reading. Using this free service, authors can make their results available to the community, in citable form, before we publish the edited article. This *Accepted Manuscript* will be replaced by the edited, formatted and paginated article as soon as this is available.

You can find more information about *Accepted Manuscripts* in the [Information for Authors](#).

Please note that technical editing may introduce minor changes to the text and/or graphics, which may alter content. The journal's standard [Terms & Conditions](#) and the [Ethical guidelines](#) still apply. In no event shall the Royal Society of Chemistry be held responsible for any errors or omissions in this *Accepted Manuscript* or any consequences arising from the use of any information it contains.

1 **Spacer-enhanced chymotrypsin-activated peptide-functionalized gold**  
2 **nanoparticles probes: a rapid assay for the diagnosis of pancreatitis**  
3

4 **Fang-Yuan Yeh<sup>1</sup>, I-Hua Tseng<sup>1</sup>, Shu-Hung Chuang<sup>1,2</sup>, Chih-Sheng Lin<sup>1, \*</sup>**

5 *1. Department of Biological Science and Technology, National Chiao Tung University,*  
6 *Hsinchu, Taiwan*

7 *2. Department of Surgery, Mackay Memorial Hospital, Hsinchu Branch, Hsinchu,*  
8 *Taiwan*

9  
10 **Running title:** Spacer-enhanced chymotrypsin-activated AuNPs-peptide probes  
11

12 **\* Author for correspondence:**

13 Chih-Sheng Lin, Ph.D.  
14 Department of Biological Science and Technology,  
15 National Chiao Tung University,  
16 No.75 Po-Ai Street, Hsinchu 300, Taiwan  
17 Tel: 886-3-5131338  
18 E-mail: [lincs@mail.nctu.edu.tw](mailto:lincs@mail.nctu.edu.tw)

## 1 **Abstract**

2 Pancreatitis is the inflammation of the pancreas. Chymotrypsin, an indicator of  
3 pancreatic function, could serve as a biomarker for the diagnosis of pancreatitis. A gold  
4 nanoparticles (AuNPs)-based fluorescence assay was fabricated in this study to assay  
5 the activity of chymotrypsin. Peptides labeled with fluorophore were conjugated onto  
6 AuNPs as chymotrypsin-activated peptide-functionalized AuNPs probe (AuNPs-peptide  
7 probe). The detection sensitivity of the AuNPs-peptide probe toward proteolytic activity  
8 was significantly increased by using spacer-enhanced peptides with specifically  
9 designed lengths and charges. The limit of detection of the designed AuNPs-peptide  
10 probe decreased, enabling detection at the pM level within a 15 min detection time.

11 The AuNPs-peptide probe was used to evaluate chymotrypsin activity as an  
12 indicator of acute pancreatitis (AP) in a mouse model induced by cerulein challenge.  
13 The fecal chymotrypsin activity in cerulein-induced AP mice was significantly lower  
14 than that observed in controls. This is the first study to use an AuNPs-peptide probe for  
15 the diagnosis of pancreatitis using fecal specimens.

16

17 **Keywords:** chymotrypsin; gold nanoparticles; peptide, pancreatitis; molecular probe

## 18 **1. Introduction**

19 Pancreatitis is a disease in which the pancreas experiences under inflammation. It  
20 occurs when digestive enzymes are activated before they are secreted into the  
21 duodenum, allowing them to attack and damage the pancreas. In the United States, at  
22 least 250,000 patients are admitted to the hospital each year for acute pancreatitis (AP),  
23 making it the second most common gastrointestinal disease. The incidence of  
24 pancreatitis continues to increase each year. The annual cost of caring for these patients  
25 is approximately \$4 – \$6 billion <sup>1</sup>. Although the pathogenesis of AP is not fully  
26 understood, most hypotheses are based on the concept of the premature activation of  
27 digestive zymogens in the pancreas, leading to tissue necrosis by auto-digestion <sup>2</sup>.  
28 Measurements of plasma amylase and lipase levels are the most widely used methods  
29 for AP diagnosis <sup>3,4</sup>. However, false-positive amylase and lipase results could be caused  
30 by abnormal conditions <sup>5</sup>, and false-negative results could be obtained in hyperlipidemia  
31 <sup>6</sup> or diabetic ketoacidosis <sup>7,8</sup>. Furthermore, blood enzyme determinations are invasive  
32 tube tests that are not routinely available for use in the diagnosis of AP. Therefore,  
33 biochemical tests based on a single fecal sample serve can as a potential and valuable  
34 diagnostic alternative <sup>9</sup>. Although trypsin preactivation is the principal cause of  
35 pancreatitis, trypsin undergoes degradation in the distal small bowel, which make  
36 trypsin a bad fecal marker <sup>10</sup>. Previous studies have shown that chymotrypsin can serve  
37 as an indicator of pancreatic function and be related to pancreatic diseases <sup>11,12</sup>.  
38 Chymotrypsin is a serine protease secreted from the pancreas into the duodenum, where  
39 it becomes active. In the case of pancreas insufficiency secondary to pancreatitis, the  
40 secretion of the enzyme is markedly reduced; therefore, reduced chymotrypsin activity  
41 can be measured in pancreatitis. As with all fecal protease assays in conventional

42 pancreatic function tests, fecal chymotrypsin can be utilized as a surrogate <sup>13</sup>. In the past  
43 few decades, reports have described various proteases assays that are primarily based on  
44 liquid chromatography, substrate zymography, enzyme-linked immunosorbent assays  
45 (ELISA), radioisotopes, or chromogenic and fluorogenic substrates. However, these  
46 techniques are often associated with cost-ineffective features such as being  
47 time-consuming, expensive, discontinuous, or requiring specific instruments. Much  
48 attention has been paid to resonance energy transfer (RET) for *in vitro* and *in vivo*  
49 assays of proteases due to advances in fluorescence-based techniques <sup>14-16</sup>. Gold  
50 nanoparticles (AuNPs) are a potential nanomaterial for RET-based assays; AuNPs of  
51 less than 40 nm in diameter have the lowest scattering constant and therefore the highest  
52 potential to quench fluorescence <sup>17</sup>. AuNPs have a superior quenching efficiency in a  
53 broad range of wavelengths compared to other organic quenchers <sup>17,18</sup>.

54 We aimed to develop an efficient method to diagnose pancreatic disease by fecal  
55 samples. Therefore, AuNPs-peptide probes for the detection of chymotrypsin activity  
56 were fabricated. The FITC-labeled peptides were conjugated onto AuNPs as  
57 chymotrypsin-activated peptide-functionalized AuNPs probe (*i.e.*, AuNPs-peptide  
58 probe), and a specially designed peptide spacer that could significantly increase the  
59 detection sensitivity was also introduced. The chymotrypsin activity in the feces of  
60 cerulein-induced AP mice was detected, and the results confirmed that the fabricated  
61 AuNPs-peptide probe could be effectively applied to the diagnosis of pancreatitis.

62

63

64

65

## 66 **2. Results**

### 67 **2-1. Fabrication of chymotrypsin-activated peptide-functionalized AuNPs probes**

68 The fabrication of the protease-activated AuNPs-peptide probes is illustrated in **Fig.**  
69 **1A**. In each probe, specific FITC labeled peptides were self-assembled onto AuNPs  
70 through an Au-S bond by cysteine-gold interaction, of which Cys acted as an anchor.  
71 The fluorescence of FITC is quenched by AuNPs, and the fluorescence can only be  
72 recovered by protease activation, which hydrolyzes the peptide substrates allows FITC  
73 to diffuse beyond the efficient quenching distance from the nanoparticles. Fluorescence  
74 was measured using excitation/emission at 495/515 nm, and the change in fluorescence  
75 intensity was used to estimate protease activity.

### 77 **2-2. Characteristics of the AuNPs-peptide probes**

78 The sizes of the synthesized citrate-capped AuNPs were estimated by TEM to be  
79  $14.6 \pm 2.4$  nm (**Fig. 1B**) and by dynamic light scattering (DLS) to be 22 nm (**Fig. 1C**).  
80 The size of the AuNPs-P3 probe was estimated by TEM (**Fig. 1D**) and DLS (**Fig. 1E**) as  
81  $17.2 \pm 1.1$  nm and 29 nm in diameter, respectively. The citrate-capped AuNP and  
82 AuNPs-peptide probe demonstrated absorption spectra with a localized surface plasmon  
83 resonance (LSPR) band shift, with the absorption peak shifted from 520 to 525 nm (**Fig.**  
84 **1F**). The chymotrypsin-activated AuNPs-peptide probe showed a similar absorption  
85 spectrum to that of the with non-activated AuNPs-peptide probe.

86 Agarose gel electrophoresis was performed to identify the morphological changes  
87 in the AuNPs after fabrication and protease activation. Changes in the bands could be  
88 observed under visible light and UV-illumination. The gel shown in **Fig. 2A** (under  
89 visible light) indicates differences in migration between the citrate-capped AuNPs, the

90 AuNPs-peptide probe, and the chymotrypsin-activated AuNPs-peptide probe. The  
91 UV-illuminated fluorescence band of the AuNPs-peptide probe without chymotrypsin  
92 activation was very weak; evidence for both free and bound peptide-FITC cleaved by  
93 chymotrypsin are also given in **Fig. 2B** (under UV-illumination).

94

### 95 **2-3. Chymotrypsin activity assay by the AuNPs-peptide probes**

96 AuNPs fabricated with different peptide substrates (listed in **Table 1**) were  
97 compared. Three fabricated AuNPs-peptide probes were used in the chymotrypsin  
98 activity assay with a 1 h detection time at 37°C and pH 8.0. As shown in **Fig. 2C**, the  
99 recovered fluorescence intensity upon chymotrypsin activation was in the following  
100 decreasing order: AuNPs-P3 probe (6000 a.u.) > AuNPs-P2 probe (3000 a.u.) >  
101 AuNPs-P1 probe (500 a.u.). Notably, only 5 ng mL<sup>-1</sup> chymotrypsin was applied to the  
102 AuNPs-P3 probe, whereas 500 ng mL<sup>-1</sup> chymotrypsin was applied to the others. Further  
103 investigation of the optimal detection range and time are documented in **Table 1**. The  
104 required optimal detection time for each AuNPs-peptide probe decreased in the  
105 following order: AuNPs-P1 probe (60 min) > AuNPs-P2 probe (30 min) > AuNPs-P3  
106 probe (15 min). Because the AuNPs-P3 probe showed superior sensitivity, the following  
107 experiments were conducted with this specific probe only.

108 To optimize the fluorescence assays using the AuNPs-peptide probe, the  
109 AuNPs-peptide probe concentration was a prime concern because the quenching effect  
110 of AuNPs is distance dependent. The concentration will affect the distance between  
111 particles, and that the adjacent particles can participate in quenching fluorescence of  
112 FITC. Different concentrations of the AuNPs-P3 probe (0.156 – 3.75 nM) were  
113 incubated with a fixed concentration of chymotrypsin (7.5 ng mL<sup>-1</sup>) for 15 min at 37°C.

114 **Fig. 3A** shows that the optimal concentrations range of the AuNPs-peptide probe was  
115 0.625 – 1.25 nM, whereas higher or lower concentrations resulted in poor performance,  
116 as indicated by the minor change in fluorescence intensity.

117 The specificity of the AuNPs-peptide probe was also investigated by comparing the  
118 use of serine proteases such as trypsin and chymotrypsin. Trypsin has a cleavage site at  
119 arginine (Arg) in P3. The AuNPs-P3 probe (1.25 nM) was incubated with various  
120 concentrations of trypsin and chymotrypsin (0.25 – 25 ng mL<sup>-1</sup>), respectively, for 15  
121 min at 37°C and pH 8.0. **Fig. 3B** shows that the AuNPs-peptide probe was highly  
122 specific to chymotrypsin and displayed almost no change in fluorescence intensity in  
123 the presence of trypsin.

124 The time-dependent emission spectrum of the AuNPs-P3 probe upon treatment  
125 with 200 pM chymotrypsin is shown in **Fig. 4A**. The results indicated that the  
126 fluorescence intensity reached a steady state after approximately 80 min at 37°C. The  
127 reaction kinetics of the AuNPs-P3 probe and chymotrypsin is an important parameter to  
128 in determining its biological applicability. To obtain the kinetic parameters, the  
129 fluorescence signal at 515 nm was plotted as a function of time (**Fig. 4A**, left). The  
130 pseudo-first-order rate,  $k_{\text{obs}}$ , was found to be 0.0424 s<sup>-1</sup> by fitting the delta fluorescence  
131 intensity data with a single exponential function. The best fit with a single exponential  
132 function gave a  $t_{1/2}$  of 16.3 min. Therefore, the detection time of the chymotrypsin assay  
133 using the AuNPs-P3 probe was determined to be 15 min. The concentration correlation  
134 was also displayed in **Fig. 4B**, where the AuNPs-P3 probe (1.25 nM) was incubated  
135 with various concentrations of chymotrypsin (0.1 – 25 ng mL<sup>-1</sup>) for 15 min at 37°C and  
136 pH 8.0. The results showed higher fluorescence intensities with increasing  
137 concentrations of chymotrypsin (**Fig. 4B**, right). The linear response to chymotrypsin,

138 from 0.25 to 10 ng mL<sup>-1</sup>, was well defined, with  $\Delta$  FL intensity = 506.69 (chymotrypsin)  
139 – 90.82 and  $R^2 = 0.99$  (**Fig. 4B**, left).

140 The stability of the AuNPs-peptide probes was evaluated and the results showed  
141 that the chymotrypsin assay using the AuNPs-P3 probe after 1 month of storage at  
142 ambient temperature was still above 90% compared to fresh use (data not shown).

143

#### 144 **2-4. Cerulein-induced AP mice**

145 AP induction in the mouse model was conducted by a series of intraperitoneal  
146 cerulein injections. The mice were sacrificed at 8, 10, or 24 h after the first  
147 administration of saline (as control) or cerulein.

148 The collected plasma was analyzed by a Fujifilm clinical chemistry analyzer, in  
149 which of the amylase and lipase levels were determined. The plasma amylase levels of  
150 the cerulein-induced group were 27 and 49 (10<sup>3</sup> U L<sup>-1</sup>) at the 8<sup>th</sup> and 10<sup>th</sup> h of sacrifice,  
151 respectively, which were significantly higher than of the values from the saline group  
152 (**Fig. 5A**). Moreover, the plasma lipase levels showed the same trend in the  
153 cerulein-induced group, with levels of 2.3 and 3.4 (10<sup>3</sup> U L<sup>-1</sup>) at the 8<sup>th</sup> and 10<sup>th</sup> h of  
154 sacrifice, respectively, also significantly higher than of the values for the saline group  
155 (**Fig. 5B**). The saline group in each sacrificed period showed the similar amounts of  
156 plasma amylase (approximately 4,000 U L<sup>-1</sup>) and lipase (approximately 500 U L<sup>-1</sup>) in  
157 each period. Both the plasma amylase and lipase levels showed at least a 3-fold increase  
158 compared to the controls, indicating that AP induction was successful in this study.

159 The pancreatic tissues of the mice were collected to confirm trypsin preactivation  
160 in AP occurrence. Extreme caution was exercised during the isolation of the pancreas  
161 because these tissues can be easily confused with fatty tissue (**Supplemental Fig. S1A**),

162 and beta cells can be identified by dithizone (DTZ) staining (**Supplemental Fig. S1B**  
163 and **S1C**). The AuNPs-P3 probe was used to analyze pre-activated chymotrypsin in the  
164 pancreas. **Fig. 5C** shows that the pancreatic chymotrypsin level in the mice with  
165 cerulein-induced AP was approximately 2.8 – 3.6 ng chymotrypsin mg<sup>-1</sup> total protein,  
166 which was significantly higher than that observed in the control group.

167

## 168 **2-5. Diagnosis of AP by duodenal and fecal chymotrypsin**

169 The collected eluent from the duodenum was analyzed using the AuNPs-P3 probe  
170 to determine the level of chymotrypsin. The amount of duodenal chymotrypsin in the  
171 mice with cerulein-induced AP showed a significant decrease in all three periods  
172 compared with that of the control group (**Fig. 6A**). The normal level of chymotrypsin  
173 was approximately 45 µg in the duodenal eluent, and significantly decreased to  
174 approximately 10 µg in the cerulein-induced group.

175 Fecal sample collection was conducted in 1 h-intervals for the entire 24 h time  
176 course. The supernatant collected from the fecal protein extraction was applied to the  
177 AuNPs-P3 probe (1.25 nM). Every 5 h period was classified into one group, thus  
178 generating the following groups: 0 – 4<sup>th</sup> h, 5 – 9<sup>th</sup> h, 10 – 14<sup>th</sup> h, 15 – 19<sup>th</sup> h and 20 – 24<sup>th</sup>  
179 h. The saline subjects showed changes in the cycle of chymotrypsin activity due to their  
180 diet. The 0 – 4<sup>th</sup> h, 5 – 9<sup>th</sup> h and 20 – 24<sup>th</sup> h groups from the mice with cerulein-induced  
181 AP showed a significantly lower chymotrypsin level compared with those of the control  
182 group (**Fig. 6B**).

183

184

185

### 186 3. Discussion

#### 187 3-1. Fabrication of AuNPs-peptide probes

188 The use of protease-activatable fluorophore-conjugated AuNP probes has recently  
189 attracted considerable attention for the development of high-sensitivity detection  
190 methods for physiological activities. AuNPs 15 nm in size offer a high potential to  
191 quench fluorescence<sup>17</sup>; therefore, 15 nm AuNPs were used in this study, and  
192 fluorophores such as FITC, were conjugated to the terminus of the peptide substrates.  
193 The relationship between the AuNPs and the fluorophore is complex at very close  
194 distances ( $< 10 \text{ \AA}$ ), radiative rate enhancement dominates; at intermediate distances (20  
195  $- 300 \text{ \AA}$ ), energy transfer is the dominant process; and at very large distances ( $> 500 \text{ \AA}$ ),  
196 fluorescence oscillations due to dipole-mirror effects take precedence<sup>19</sup>. According to  
197 the size analysis results that the distance between AuNPs and FITC was approximately  
198  $13 - 35 \text{ \AA}$ , indicating quenching mechanism dominates this system. Based on the  
199 nanometal surface energy transfer model, the quantum efficiency of the AuNPs-P3  
200 probe was approximately  $88.3 - 99.7\%$ , theoretically<sup>20</sup>. The enzyme activity was  
201 determined by the recovered fluorescence, which was defined as the difference between  
202 the experiment group and the control group; hence the delta fluorescence intensity was  
203 able to eliminate the background effect.

204 The importance of peptide sequence design for the ligands coated on AuNPs has  
205 been previously studied<sup>21</sup>, because of the citrate-capped AuNPs showed poor stability  
206 (as shown in **Supplemental Fig. S2B**). For a targetable probe used to detect protease  
207 activity, the peptide sequence must be limited to specific hydrolysis substrates.  
208 Therefore, it is essential to consider the overall effect of the peptide rather than only  
209 effect of the particular amino acid. It has been previously shown that increasing the

210 length of the peptide can increase the stability of peptide-capped AuNPs<sup>22</sup>. Moreover, a  
211 previous study also proposed that peptide-modified AuNPs aggregation can be  
212 controlled by electrostatic repulsion between the peptides<sup>23</sup>. The aim of peptide design  
213 is to efficiently decrease the steric barrier caused by the densely packed layer of  
214 peptides on the AuNP surface to increase enzyme access to the cleavage site. Hence,  
215 this study examined two main concepts in peptide design, namely, length and charge.  
216 Three different peptide substrates were compared, with each possessing the same  
217 cleavage sites for chymotrypsin (**Table 1**). The length was tailored through the use of a  
218 spacer of repeating Gly units, (Gly)<sub>5</sub> (the difference between P1 and P2), and the charge  
219 was modified by substituting the non-charged (Gly)<sub>5</sub> spacer with a negatively-charged  
220 (Asp)<sub>5</sub> spacer (the difference between P2 and P3). The pH was adjusted according to the  
221 isoelectric point (pI) of the peptides to achieve a net negative charge on the peptide;  
222 hence to stabilize the AuNPs-peptide probe (data not shown). Besides, the pH of the  
223 AuNPs had no effect on aggregation (**Supplemental Fig. S2A**).

224 AuNPs fabricated with peptide ligands can improve the stability of particles<sup>24</sup>, but  
225 the AuNPs-P2 probe stability showed was worse than that of the citrate-capped AuNPs  
226 (**Supplemental Fig. S2C**). Nevertheless, the use of a stabilizer such as BSA, efficiently  
227 increased the stability of the AuNPs-P2 probe (data not shown). The negatively-charged  
228 spacer, (Asp)<sub>5</sub>, promoted electrostatic repulsion between the particles and increased the  
229 stability of the AuNPs, which show good dispersion (**Supplemental Fig. S2D**).

230 DTT-based displacement was conducted to estimate the number of peptides conjugated  
231 to each AuNP. Our results showed that the number of peptide substrates (9 – 13  
232 residues) conjugated to the 15 nm AuNPs was approximately 1,000 – 1,800 peptides per  
233 AuNP or 2.5 – 1.5 peptides nm<sup>-2</sup>. Compared with previous reports involving a short

234 peptide (2 – 6 residues) found approximately 200 – 900 peptides per AuNP 12 – 12.5  
235 nm in size, our results showed a higher conjugation ratio<sup>22, 25, 26</sup>. In other words, the  
236 synthesized AuNPs-peptide probes were compactly packed with peptides. The  
237 advantages of the densely packed monolayers are as follows: (1) more loading peptides  
238 provide more chances for proteases to hydrolyze and activate the AuNPs-peptide probes,  
239 and (2) compact coverage increase the stability of AuNPs-peptide probes compared to  
240 that of citrate-capped AuNPs.

241 The zeta potential indicates the degree of repulsion between adjacent, similarly  
242 charged particles in dispersion. Colloids with a high zeta potential (negative or positive)  
243 are electrically stabilized, whereas those with low zeta potentials tend to coagulate or  
244 flocculate. A value of 25 mV (positive or negative) can be taken as the arbitrary value  
245 separating lowly-charged surfaces from highly-charged surfaces<sup>27</sup>. Park et al. showed  
246 that the zeta-potential value of AuNP to AuNPs-peptide-fluorescent protein changed  
247 from  $-26.44 \pm 2.58$  mV to  $5.46 \pm 2.44$  mV<sup>28</sup>. Compared with our results, this value is  
248 less stable. The zeta potentials of the citrate-capped AuNPs and AuNPs-P3 probe in our  
249 study increased from  $-34.7 \pm 13.8$  mV to  $-39.2 \pm 15.9$  mV; this improvement can be  
250 attributed to the (Asp)<sub>5</sub> spacer.

251

### 252 **3-2. Establishment of chymotrypsin activity assay using the AuNPs-peptide probe**

253 A review of AuNPs-based biosensors for enzyme activity documented that the  
254 number of published AuNPs-based protease assays is relatively low (< 100 publications)  
255 and only a few proteases (kinases, MMPs, and caspases) have appeared frequently to  
256 date<sup>29</sup>. This study presents a new target for AuNPs-based protease assays and a novel  
257 investigation of the effect of spacer length and charge on sensitivity. The specially

258 designed peptide chain consisted of four elements: an anchor, a spacer, a sequence  
259 hydrolyzed by proteases, and a fluorophore. According to the results presented in **Fig.**  
260 **2C**, the three fabricated probes showed different sensitivities in detecting chymotrypsin.  
261 The AuNPs-P2 probe showed a 5-fold increase in the delta fluorescence intensity  
262 compared to that observed in the AuNPs-P1 probe. It has been demonstrated that longer  
263 spacers on gold glyconanoparticles, which are AuNPs modified with a variety of  
264 saccharide molecules, enhance binding affinity to the target (lectins)<sup>30</sup>. The results also  
265 corresponded to our observation that a longer spacer could result in a larger distance  
266 between the ligands at the same ligand density, hence reducing steric hindrance when  
267 the target approaches the ligands, making the ligands more accessible for interaction  
268 with the target.

269 The detection sensitivity of the AuNPs-P3 probe was superior (>100-fold)  
270 compared to that of the AuNPs-P2 probe. In our study, we proposed that the (Asp)<sub>5</sub>  
271 residues played a novel role as an extending anchor that decreased the steric hindrance  
272 to the enzyme and lowered the pI of the peptide, increasing particle stability. Asp also  
273 excluded the adsorbed citrate on the AuNP, due to its repulsive interactions with the  
274 citrate carboxylates<sup>22</sup>. Hence, the repulsions between the chains and the citrate ions on  
275 the surfaces of the AuNPs maintained the dispersion of the peptides. The mechanism  
276 behind the increase in sensitivity using of a charged peptide spacer in functionalized  
277 AuNP-peptide probes remains to be explored. A few studies have shown that an  
278 enhancement of enzyme activity is possible using nanoparticles modified with  
279 polyvalent-conjugates. (Arg)<sub>6</sub> was used in the generation of cationic peptide formed  
280 nanoparticles that possessed significantly enhanced antimicrobial properties<sup>31</sup>.  
281 Functionalized dextranated magnetic nanoparticles with different valency of small

282 molecules have shown an over  $10^4$ -fold increase in avidity to the molecule-binding  
283 protein<sup>32</sup>. Algar et al. have previously demonstrated that an increase in the charge of  
284 polyvalent QD-peptide conjugates can significantly enhance the sensitivity to trypsin  
285 cleavage of the peptide conjugates<sup>33</sup>. To the best of our knowledge, this study is the  
286 first report of the use of polyvalent peptide spacers to enhance enzyme activity in a  
287 AuNPs-based system for proteinase activity determination.

288 The enhancement of enzyme sensitivity through the use of spacers might also be  
289 due to the electrostatic complementarity between (Asp)<sub>5</sub> and chymotrypsin. A previous  
290 study showed that anionic functionalized nanoparticles were highly effective  
291 surface-based inhibitors of chymotrypsin; this activity was attributed to the electrostatic  
292 complementarity between the carboxylate end groups and the halo of cationic residues  
293 located around the periphery of the active site in chymotrypsin<sup>34</sup>.

294 Morphological changes in AuNPs with different treatments can be observed by  
295 agarose gel electrophoresis<sup>35</sup>. The mobility of the citrate-capped AuNPs increased upon  
296 modification with negatively-charged peptides, namely, the AuNPs-peptide probe. The  
297 mobility was further increased in the chymotrypsin activated AuNPs-peptide probe due  
298 to the loss of residues (**Fig. 2A**). The quenching phenomenon between AuNPs and FITC  
299 is confirmed in **Fig. 2B**; chymotrypsin activation is shown to turn on the fluorescence.  
300 The UV-illuminated gel shows that the fluorescent band with poorer mobility was  
301 attributed to the loss of the (Asp)<sub>5</sub> residues (Lane 4 and Lane 5). The quenching effect  
302 of AuNPs is very important; therefore, the concentration of the AuNPs-peptide probe  
303 was considered due to its influence on the distance between individual particles. **Fig. 3A**  
304 shows the optimal concentration range; higher or lower concentrations led to smaller  
305 changes in fluorescence intensity, and higher concentrations especially resulted in

306 considerable decreases in intensity. The higher concentration likely had a negative  
307 impact due to the quenching effect whereas the lower concentration likely provided  
308 insufficient loading of the peptide substrates to detect protease activity. Additionally, the  
309 specificity of the AuNPs-peptide probe was investigated using the serine protease  
310 trypsin. Trypsin was chosen because it is structurally similar to chymotrypsin and  
311 follows the same secretion route in the digestive system. Trypsin has one cleavage site  
312 in the peptide substrate (P3); however, **Fig. 3B** shows that the AuNPs-peptide probe was  
313 unable to detect trypsin but exhibited high specificity to chymotrypsin.

314

### 315 **3-3. Application of AuNPs-peptide probe to the diagnosis of AP**

316 The AP mouse model was successfully established in this study (**Supplemental**  
317 **S3**). Mice with cerulein-induced AP showed increased levels of plasma amylase and  
318 lipase. We aimed to confirm the presence of premature trypsin in AP based on increased  
319 pancreatic chymotrypsin activity<sup>36</sup>. Pancreatic acinar cells produce the inactive  
320 precursor of chymotrypsin, chymotrypsinogen, which is carried in the pancreatic juice  
321 through the pancreatic duct into the duodenum and then activated by trypsin. The  
322 chymotrypsin activity in the pancreas of cerulein-induced AP mice was analyzed by the  
323 AuNPs-P3 probe because of their high sensitivity. **Fig. 5C** supports the hypothesis that  
324 pancreatic chymotrypsin activity is significantly increased in mice with  
325 cerulein-induced AP, with chymotrypsin activity found to be increased by 3-fold  
326 compared to that of in the controls. Few works have discussed the elevated activity of  
327 chymotrypsin in the pancreas with AP. In a cerulein-induced rat model, a 3-fold  
328 increase in chymotrypsin activity has been observed relative to the normal reference<sup>36</sup>,  
329 which is consistent with our results. The reported maximal pancreatic injury at the 12<sup>th</sup> h

330 <sup>37</sup> was also similar to our findings that the 10<sup>th</sup> h showed the highest level of pancreatic  
331 chymotrypsin.

332 However, there were inconsistencies in the pancreatic chymotrypsin, plasma  
333 amylase and lipase activity levels at the 24<sup>th</sup> period, at which time levels of pancreatic  
334 chymotrypsin remained abnormal, whereas the other enzymes had reached normal  
335 levels. We were thus prompted to examine the two sources of chymotrypsin secretion.  
336 Chymotrypsin activity as an indicator to estimate the occurrence of pancreatitis usually  
337 refers to fecal chymotrypsin <sup>12</sup>; however, the chymotrypsin in duodenal fluid was also  
338 investigated in this study. The duodenal contents of cerulein-induced AP mice were  
339 collected after proper fasting to exclude the effect of food. The amount of chymotrypsin  
340 in mice with cerulein-induced AP significantly decreased in the duodenal fluid in all  
341 periods compared with that of the saline subjects (**Fig. 6A**). The duodenal chymotrypsin  
342 activity in mice with cerulein-induced AP showed a 25% decrease relative to that of  
343 controls. Acinar cell injury leads to pancreas malfunction, resulting in a decrease in  
344 chymotrypsin activity in the duodenum. This study is the first report to investigate the  
345 potential of duodenal chymotrypsin as a reliable index for AP in a mouse model. The  
346 duodenal chymotrypsin activity provides a direct estimate of pancreatic injury; however,  
347 it offers one disadvantage in that it is invasive to obtain duodenal fluid. But for broader  
348 applications, the AuNPs-peptide probe has the potential in surgical applications,  
349 allowing real-time visualization of pancreatic juice leakage during surgery <sup>38</sup>.

350 Normally, for clinical diagnosis, 24 to 72 h stool collection is needed for protease  
351 determination <sup>12, 39</sup>. The use of fecal chymotrypsin as an indicator of pancreatitis  
352 diagnosis usually refers to chronic pancreatitis; hence, we tried to find the applicability  
353 in acute pancreatitis. For stool productive species like mouse, that one collection of

354 stool is not reasonable for experimental design; therefore, we conducted a 24 h  
355 collection of stool with 1-h intervals. Intra peritoneal cerulein injection can cause  
356 stomachache and loss of appetite; hence, fasting beforehand might encourage the mice  
357 to eat and therefore to produce stool. A continuous 24 h stool collection not only  
358 provided a time course for mouse digestion but also showed the change of fecal  
359 chymotrypsin activity in the mouse model of AP. Because of individual and digestion  
360 rate differences, the 24 h stool collection was categorized into groups to average  
361 performances. The saline subjects showed a cycle change in chymotrypsin activity due  
362 to their diet. Base on overall average, the cerulein-induced group had lower fecal  
363 chymotrypsin activity than that of controls, which the dividing fecal chymotrypsin as  
364 abnormal status was approximately  $30 \text{ ng mg}^{-1}$  of stool. Especially the 0 – 4<sup>th</sup> h, 5 – 9<sup>th</sup>  
365 h and 20 – 24<sup>th</sup> h groups of cerulein-induced AP mice showed significantly lower fecal  
366 chymotrypsin activity (30%) relative to that of controls (**Fig. 6B**). It has been proposed  
367 that a fecal chymotrypsin below  $3 \text{ U g}^{-1}$  of stool (approximately  $75 \text{ ng mg}^{-1}$  of stool)  
368 suggests advanced chronic pancreatitis in human<sup>40</sup>. The advantage of fecal  
369 chymotrypsin over duodenal chymotrypsin is its ease of specimen collection. Moreover,  
370 based on the high sensitivity of the AuNPs-P3 probe, only 10 – 20 mg of feces is  
371 required for the assay, making monitoring feasible.

372

373

## 374 **4. Experimental section**

### 375 **4-1. Chemicals**

376 All chemicals were analytical reagent grade and used without further purification.

377 Sodium citrate ( $\text{C}_6\text{H}_5\text{Na}_3\text{O}_7 \cdot 2\text{H}_2\text{O}$ ), calcium chloride ( $\text{CaCl}_2$ ), Triton X-100, hydrogen

378 tetrachloroaurate (III) ( $\text{HAuCl}_4 \cdot 3\text{H}_2\text{O}$ ), Brij™ 35 solution 30% (w/v), polyethylene  
379 glycol (#P2139, Mw 8000), DL-dithiothreitol (#D5545), dithizone (#D5130),  
380 collagenase type I (#C9891), chymotrypsin (#C4129) were obtained from  
381 Sigma-Aldrich (St. Louis, MO, USA). HPLC-grade acetonitrile (ACN), were obtained  
382 from Merck (Darmstadt, Germany). Tris-HCl, dulbecco's phosphate buffered saline  
383 (DPBS), were purchased from Invitrogen (San Diego, LA, USA). Sodium chloride was  
384 purchased from USB (Cleveland, OH, USA). Nanopure water (18 M $\Omega$ •cm; Millipore,  
385 Bedford, MA, USA) was used in all experiments and to prepare all buffers.

386

#### 387 **4-2. Apparatus**

388 Absorption spectra of AuNPs and fabricated-AuNPs were analyzed by UV-Vis  
389 spectrophotometer (SpectraMax 190; Molecular Devices Corporation, Sunnydale, CA,  
390 USA). Absorbance values of protein assay were recorded at 595 nm using a UV-Vis  
391 spectrophotometer (Molecular Devices Corporation). The fluorescence signals of  
392 AuNPs-peptide probe were analyzed by fluorescence spectrophotometer (F-2700;  
393 Hitachi, Tokyo, Japan). Enzyme activities in plasma/serum were analyzed by Fujifilm  
394 clinical chemistry analyzer (FUJI DRI-CHEM 3500; Fujifilm Corporation; Tokyo,  
395 Japan). The gel electrophoresis analyses were performed with horizontal electrophoresis  
396 system (Mini-Sub Cell GT; Biorad, Corston, UK). Microscope equipped with a  
397 high-resolution video camera (BX51; Olympus, Tokyo, Japan). Size examination of  
398 AuNPs and fabricated-AuNPs were examined by transmission electron microscopy,  
399 TEM (JEM-1230; JEOL, Tokyo, Japan) operated at 100 kV and equipped with CCD  
400 camera, and dynamic light scattering, DLS (Brookhaven Instruments Corporation,  
401 Holtsville, NY, USA). Particles analyzed by Zetasizer Nano (Malvern Instruments,

402 Worchestershire, UK) and use disposable solvent resistant micro cuvette (ZEN0040) at  
403 room temperature.

404

#### 405 **4-3. Preparation of AuNPs**

406 AuNPs were prepared by citrate reduction method according to the reported  
407 procedure<sup>35,41</sup>. Colloidal AuNPs (15 nm in diameter) were prepared as follows: 50 mL  
408 of 1 mM chloroauric acid solution was heated with oil bath till boiling, and followed by  
409 the addition of 5 mL of 38.8 mM sodium citrate solution. The color of the solution  
410 would turn from yellow to color less to black and to wine red. After the solution was  
411 cooled to room temperature, the product of 15 nm AuNPs solution was preserved at 4°C.  
412 The size of AuNPs was confirmed by TEM and DLS, and the concentration was  
413 estimated by Beer's law with absorbent peak at 520 nm with an extinction coefficient of  
414  $3.94 \times 10^8 \text{ M}^{-1} \text{ cm}^{-1}$ .

415

#### 416 **4-4. Preparation of AuNPs-peptide probes**

417 Three peptide substrates were used in the protease activated AuNPs-peptide probes  
418 and the sequences were documented in **Table 1**. The difference between peptide#1 (P1,  
419 GPLGLAG(Hyp)C) and peptide#2 (P2, GPLGLARGGGGGC) is length which the  
420 anchor increase with a spacer of repeating glycine, (Gly)<sub>5</sub>. The difference between P2  
421 and peptide#3 (P3, GPLGLARDDDDDC) is the spacer of non-charged (Gly)<sub>5</sub> to  
422 negatively-charged aspartic acid, (Asp)<sub>5</sub>. However, three of them have the same  
423 cleavage sites to chymotrypsin. The peptide-FITC was synthesized commercially by  
424 Genesis Biotech (Taipei, Taiwan). The peptide included a cysteine (Cys) in the  
425 C-terminal containing a thiol group (-SH) which could conjugate on to AuNPs through

426 Au-S bond. The probes were synthesized as following: the prepared AuNPs were  
427 adjusted to proper pH by 1 N HCl or 1 N NaOH and then the concentration was  
428 adjusted with ddH<sub>2</sub>O to OD = 1, which was 980  $\mu$ L of 2.5 nM AuNPs. AuNPs were  
429 mixed with 10  $\mu$ L of 1 mg mL<sup>-1</sup> peptide-FITC and 10  $\mu$ L of 0.01 M phosphate buffer  
430 containing 0.1% SDS and 0.3 M NaCl, and then the mixture were shaken for 12 h, 40  $\times$   
431 g at room temperature. AuNPs-peptide probes were purified by two rounds of  
432 centrifugation. After first centrifugation (10,000  $\times$  g for 20 min), the supernatant was  
433 carefully removed and added 500  $\mu$ L 2% (wt/wt) PEG. After the second centrifugation  
434 (11,000  $\times$  g, for 20 min), the supernatant was removed and resuspended with ddH<sub>2</sub>O of  
435 AuNPs-P3 probe or 0.1% BSA of AuNPs-P1 and AuNPs-P2 probes.

436

#### 437 **4-5. Gel electrophoresis of AuNPs-peptide probes**

438 Gel electrophoresis analysis modified from Hanauer' protocol was used to confirm  
439 the change of AuNPs after fabrication and protease (chymotrypsin) activation<sup>40</sup>. The  
440 morphological change could be observed from visible red bands of AuNPs and  
441 UV-illuminated fluorescent bands. Agarose gels (1.5%) were used and prepared with  
442 0.5X TBE buffer. All samples loaded with 35% glycerol for increasing density as the  
443 ratio of 7:1 (in volume). The citrate-capped AuNPs mixed with very small amount of  
444 10% SDS (1  $\mu$ L) for migration. The gels were run in a horizontal electrophoresis system  
445 for 30 min at 110 V in 0.5X TBE buffer. Gel images were taken by a digital camera  
446 under visible light and UV-light; besides, the images might be processed with small  
447 linear contrast adjustments in order to obtain the true representation.

448

449

#### 450 **4-6. Dithiothreitol-based displacement**

451 Dithiothreitol (DTT)-based displacement was utilized for separating peptides from  
452 their AuNP. DTT will reactively displace the ligands from surface sites because it is  
453 much more reactive toward AuNP compared with most ligands of interest<sup>42</sup>. In this  
454 study, the conjugate ratio of peptide-FITC to AuNPs could be quantified by  
455 fluorescence intensity. Fluorescence was measured using excitation/emission of  
456 495/515 nm. DDT-based displacement was conducted as following: prepared 50 mg  
457 mL<sup>-1</sup> DTT (dissolved in pH 6.5 PB buffer, 0.1 M) and then added 500  $\mu$ L DTT to  
458 suspend AuNP probe sediment (0.625 nM) for 12 h incubation at room temperature.  
459 The total fluorescence of loading peptide substrates was defined after proper dilution  
460 and acquired a linear correlation between peptide-FITC concentration and fluorescence  
461 intensity, and the supernatant of DTT displacement also processed with same procedure  
462 to acquire the linear correlation. Dilution buffer was TTC buffer (50 mM Tris, 10 mM  
463 CaCl<sub>2</sub>, 150 mM NaCl and 0.05% Brij 35, pH 8.0).

464

#### 465 **4-7. General procedure for chymotrypsin activity measurements by**

##### 466 **AuNPs-peptide probe**

467 For the standard chymotrypsin activity assay, chymotrypsin (25 kDa) prepared in  
468 1mM HCl with 2 mM CaCl<sub>2</sub> and stored at -20°C. Different concentrations of  
469 chymotrypsin were diluted with pH 8.0 TTC buffer and added into AuNPs-peptide  
470 probe (125  $\mu$ L) to comprise 250  $\mu$ L of mixture, and then incubated at 37°C. All of the  
471 solutions were analyzed with fluorescence spectrophotometer (Hitachi F-2700), using  
472 excitation/emission at 495/515 nm. Delta fluorescence intensity is the difference of  
473 recovered fluorescence between protease-activated AuNPs-peptide probe and

474 non-activated control group.

475

#### 476 **4-8. Animals**

477 Female C57BL/6 mice, purchased from the National Laboratory Animal Center  
478 (NLAC, Taipei, Taiwan), were housed at the Laboratory Animal Center, National Chiao  
479 Tung University, under standard conditions. Female mice of 6 to 8 weeks of age were  
480 used in this study. All experimental procedures were carried out in accordance with the  
481 guidelines of the Institutional Animal Care and Use Committee of National Chiao Tung  
482 University. Every effort was made to minimize the suffering of the animals and the  
483 number of animals used.

484

#### 485 **4-9. Cerulein-induced AP mouse model**

486 The cerulein-induced AP mouse model was developed according to a previous  
487 protocol<sup>43</sup>, with minor modifications. The mice were induced to develop AP by 4 doses  
488 of intraperitoneal injections of cerulein ( $200 \mu\text{g kg}^{-1}$ ) at 2-h intervals. Each group  
489 consisted of four mice. The control subjects were equally treated with 0.9% NaCl ( $10$   
490  $\mu\text{L mg}^{-1} 2 \text{ h}^{-1}$ , 4 IP injections). The mice were sacrificed at 8, 10, or 24 h after the first  
491 administration of saline (as a control) or cerulein. Mice were fasted for 6 h prior to  
492 sacrifice, after which the blood, duodenum, and pancreas were collected.

493 For the time courses of fecal chymotrypsin in AP model experiments, the mice  
494 were divided into two groups. All mice were subjected to 12 h fasting prior to injections.  
495 AP ( $n = 4$ ) was induced by 4 doses of cerulein ( $200 \mu\text{g kg}^{-1} 2 \text{ h}^{-1}$ ), and the control  
496 subjects ( $n = 3$ ) were equally treated with 0.9% NaCl ( $10 \mu\text{L mg}^{-1} 2 \text{ h}^{-1}$ ). All feces were  
497 subjected to lysis as previously described.

**498 4-10. Sample collection**

499 For the fecal chymotrypsin assay, the feces were weighed and preserved at 4°C  
500 before extraction. The fecal protein extraction process was as follows: one feces (10 –  
501 25 mg per feces) was dissolved in 0.5 mL fecal protein extraction buffer (250 mM NaCl,  
502 50 mM CaCl<sub>2</sub>, and 0.25% Triton X-100) for 5 min with continuously mixing by vortex  
503 mixer followed by centrifugation (10,000 × g, 1 min), and then the supernatant was  
504 collected.

505 For the chymotrypsin assays in the duodenal eluent and pancreas, the mice were  
506 sacrificed with CO<sub>2</sub> inhalation. Blood was collected by direct cardiac puncture and  
507 mixed with heparin to acquire plasma after centrifugation (3,000 × g, 10 min at 4°C).  
508 The first part of the small intestine followed the demarcation set by Shang<sup>44</sup> to  
509 determine the duodenum. The duodenal contents were eluted with 1 mL DPBS and  
510 collected the eluent. The duodenal eluent was treated by centrifugation (13,000 × g, 10  
511 min at 4°C), and the supernatants were collected. The pancreas tissues were  
512 homogenized with 1 mL PRO-PREP protein extraction solution (iNtRON  
513 Biotechnology, Seongnam, South Korea). The homogenates were centrifuged at 13,000  
514 × g for 10 min at 4°C. All the supernatants were collected and stored at –80°C until  
515 further analysis. The protein concentrations of the supernatant were measured using a  
516 Bio-Rad protein assay (Bio-Rad Laboratories, Hercules, CA, USA).

517

**518 4-11. Statistical analysis**

519 All data were reported as the mean ± standard deviation (SD) for the specified  
520 number of replicates indicated in the caption. Statistical significance was determined by  
521 a two-tailed Student's t-test with 95% confidence for unpaired observations. A *p* value

522 less than 0.05 was considered to be significant.

523

524

## 525 **5. Conclusions**

526 Chymotrypsin can be used as an indicator of pancreatic function. The established  
527 AuNPs-peptide probe was used in chymotrypsin assays showing high sensitivity at the  
528  $\text{pg mL}^{-1}$  level and requiring only 15 min to detect enzyme activity. The sensitivity of the  
529 AuNPs-peptide probe was greatly increased through the use of a spacer-enhanced  
530 polyvalent peptide,  $(\text{Asp})_5$ . This process is a one-step biological recognition element  
531 assembly procedure that circumvents the use of additional stabilizers and enhances  
532 stability.

533 A cerulein-induced AP mouse model was established in this study, and the  
534 AuNPs-peptide probe was successfully used to analyze chymotrypsin activity to assess  
535 pancreatic function. The plasma amylase and lipase levels were compared to the  
536 chymotrypsin activities in the duodenal eluent, the pancreas and the feces. The increase  
537 in pancreatic chymotrypsin activity indicated the pre-activation of trypsin in AP.  
538 Meanwhile, the chymotrypsin activity in the duodenal eluent provided a direct index for  
539 the estimation of pancreatic injury, although it required an invasive procedure. The fecal  
540 chymotrypsin assay serves as a non-invasive method for the diagnosis of AP, and the  
541 fecal chymotrypsin below  $30 \text{ ng mg}^{-1}$  of stool suggests AP. The AuNPs-peptide probe  
542 was successfully applied in the rapid detection of pancreatic disease-related  
543 chymotrypsin activity. Moreover, the AuNPs-peptide probe could potentially be used to  
544 monitor the leakage of pancreatic juice during surgery to avoid postoperative pancreatic  
545 fistulas. This study also provides a platform that could be applied in the daily

546 monitoring of fecal chymotrypsin activity and is non-invasive. This is the first study to  
547 use AuNPs-peptide probes in practical disease diagnosis.

548

## 549 **6. Acknowledgments**

550 This work was supported by grants NSC 98-2313-B-009-002-MY3 and NSC  
551 101-2313-B-009 -001 -MY3 from the National Science Council of Taiwan. This paper  
552 (work) was particularly supported by the "Aiming for the Top University Program" of  
553 the National Chiao Tung University and Ministry of Education, Taiwan, R.O.C.  
554 (MMH-CT-10201).

## References

1. L. Goldman, A. I. Schafer and R. L. F. Cecil, Elsevier/Saunders, Philadelphia, 24 edn., 2012, pp. 937-944.
2. W. Halangk and M. M. Lerch, *Clinics in laboratory medicine*, 2005, 25, 1-15.
3. C. Dervenis, C. D. Johnson, C. Bassi, E. Bradley, C. W. Imrie, M. J. McMahon and I. Modlin, *International Journal of Pancreatology*, 1999, 25, 195-210.
4. J. M. Steiner, *The Veterinary clinics of North America. Small animal practice*, 2003, 33, 1181-1195.
5. P. A. Sutton, D. J. Humes, G. Purcell, J. K. Smith, F. Whiting, T. Wright, L. Morgan and D. N. Lobo, *Annals of The Royal College of Surgeons of England*, 2009, 91, 381.
6. R. W. Fallat, J. W. Vester and C. J. Glueck, *JAMA*, 1973, 225, 1331-1334.
7. E. E. Argueta and K. M. Nugent, *ICU Director*, 2013.
8. M. D. Ko, M. D. Tello, L. Catherine and M. D. Salt, 2011.
9. R. M. Ayling, *Annals of Clinical Biochemistry*, 2012, 49, 44-54.
10. N. F. Adham, B. J. Dyce, M. C. Geokas and B. J. Haverback, *The American Journal of Digestive Diseases*, 1967, 12, 1272-1276.
11. D. M. Goldberg, *Clinica Chimica Acta*, 2000, 291, 201-221.
12. I. Molinari, K. Souare, T. Lamireau, M. Fayon, C. Lemieux, A. Cassaigne and D. Montaudon, *Clinical Biochemistry*, 2004, 37, 758-763.
13. J. G. Lieb Ii and P. V. Draganov, *World journal of gastroenterology*, 2008, 14, 3149.
14. C. J. Mu, D. A. LaVan, R. S. Langer and B. R. Zetter, *ACS Nano*, 2010, 4, 1511-1520.

15. S. B. Lowe, J. A. G. Dick, B. E. Cohen and M. M. Stevens, *ACS Nano*, 2012, 6, 851-857.
16. Y. P. Kim, Y. H. Oh, E. Oh, S. Ko, M. K. Han and H. S. Kim, *Analytical Chemistry*, 2008, 80, 4634-4641.
17. M. Swierczewska, S. Lee and X. Chen, *Physical Chemistry Chemical Physics*, 2011, 13, 9929-9941.
18. K. Kang, J. Wang, J. Jasinski and S. Achilefu, *Journal of Nanobiotechnology*, 2011, 9, 1-13.
19. C. S. Yun, A. Javier, T. Jennings, M. Fisher, S. Hira, S. Peterson, B. Hopkins, N. O. Reich and G. F. Strouse, *Journal of the American Chemical Society*, 2005, 127, 3115-3119.
20. T. L. Jennings, M. P. Singh and G. F. Strouse, *Journal of the American Chemical Society*, 2006, 128, 5462-5467.
21. M. Fanun, *Colloids in biotechnology*, Taylor & Francis Group, 2010.
22. R. Lévy, N. T. K. Thanh, R. C. Doty, I. Hussain, R. J. Nichols, D. J. Schiffrin, M. Brust and D. G. Fernig, *Journal of the American Chemical Society*, 2004, 126, 10076-10084.
23. J. A. Tullman, W. F. Finney, Y. J. Lin and S. W. Bishnoi, *Plasmonics*, 2007, 2, 119-127.
24. K. M. Harkness, B. N. Turner, A. C. Agrawal, Y. Zhang, J. A. McLean and D. E. Cliffel, *Nanoscale*, 2012, 4, 3843-3851.
25. I. Olmedo, E. Araya, F. Sanz, E. Medina, J. Arbiol, P. Toledo, A. Álvarez-Lueje, E. Giralt and M. J. Kogan, *Bioconjugate Chemistry*, 2008, 19, 1154-1163.
26. S. Guerrero, J. R. Herance, S. Rojas, J. F. Mena, J. D. Gispert, G. A. Acosta, F. Albericio and M. J. Kogan, *Bioconjugate Chemistry*, 2012, 23, 399-408.

27. R. Greenwood and K. Kendall, *Journal of the European Ceramic Society*, 1999, 19, 479-488.
28. K. Park, J. Jeong and B. H. Chung, *Chemical Communications*, 2012, 48, 10547-10549.
29. E. Hutter and D. Maysinger, *Trends in Pharmacological Sciences*, 2013, 34, 497-507.
30. X. Wang, O. Ramström and M. Yan, *Analytical Chemistry*, 2010, 82, 9082-9089.
31. L. Liu, K. Xu, H. Wang, P. K. J. Tan, W. Fan, S. S. Venkatraman, L. Li and Y.-Y. Yang, *Nature nanotechnology*, 2009, 4, 457-463.
32. C. Tassa, J. L. Duffner, T. A. Lewis, R. Weissleder, S. L. Schreiber, A. N. Koehler and S. Y. Shaw, *Bioconjugate Chemistry*, 2009, 21, 14-19.
33. W. R. Algar, A. Malonoski, J. R. Deschamps, J. B. Blanco-Canosa, K. Susumu, M. H. Stewart, B. J. Johnson, P. E. Dawson and I. L. Medintz, *Nano Letters*, 2012, 12, 3793-3802.
34. N. O. Fischer, C. M. McIntosh, J. M. Simard and V. M. Rotello, *Proceedings of the National Academy of Sciences*, 2002, 99, 5018-5023.
35. Y. C. Chuang, W. T. Huang, P. H. Chiang, M. C. Tang and C. S. Lin, *Biosensors and Bioelectronics*, 2012, 32, 24-31.
36. Z. Piotrowski, P. Myśliwiec, M. Gryko, H. Ostrowska and M. Baltaziak, *Rocz Akad Med Bialymst*, 2003, 48, 61-65.
37. A. A. Aghdassi, J. Mayerle, S. Christochowitz, F. U. Weiss, M. Sandler and M. M. Lerch, *Fibrogenesis & Tissue Repair* 2011, 4.
38. S. Yamashita, M. Sakabe, T. Ishizawa, K. Hasegawa, Y. Urano and N. Kokudo, *British Journal of Surgery*, 2013, 100, 1220-1228.

39. J. G. Banwell, P. J. Leonard and R. M. F. Lobo, *Gut*, 1965, 6, 143-145.
40. J. G. Lieb and P. V. Draganov, *World journal of gastroenterology : WJG*, 2008, 14, 3149-3158.
41. Y. C. Chuang, J. C. Li, S. H. Chen, T. Y. Liu, C. H. Kuo, W. T. Huang and C. S. Lin, *Biomaterials*, 2010, 31, 6087-6095.
42. D. H. Tsai, M. P. Shelton, F. W. DelRio, S. Elzey, S. Guha, M. R. Zachariah and V. A. Hackley, *Analytical and Bioanalytical Chemistry*, 2012, 404, 3015-3023.
43. M. Tsai, C. Chen, S.-H. Chen, Y. Huang and T. Chiu, *Journal of Gastroenterology*, 2011, 46, 822-833.
44. L. Shang, N. Thirunarayanan, A. Viejo-Borbolla, A. P. Martin, M. Bogunovic, F. Marchesi, J. C. Unkeless, Y. Ho, G. C. Furtado, A. Alcamí, M. Merad, L. Mayer and S. A. Lira, *Gastroenterology*, 2009, 137, 1006-1018.e1003.

1 **Figure 1.** (A) Schematic illustration of the protease activated fluorescent  
2 self-assembled AuNPs (AuNPs-peptide probe); (B) TEM image of citrate-capped  
3 AuNPs; (C) DLS result of citrate-capped AuNPs; (D) TEM image of AuNPs-P3 probe;  
4 (E) DLS measurement of AuNPs-P3 probe; and (F) absorption spectra of  
5 citrate-capped AuNP, AuNPs-P3 probe and chymotrypsin ( $500 \text{ ng mL}^{-1}$  for 15 min at  
6  $37^\circ\text{C}$ ) activated AuNPs-P3 probe.

7  
8 **Figure 2.** (A) Agarose gel showing the migration of the bands of AuNPs and  
9 fabricated- AuNPs, which appear red in color; (B) the UV-illuminated gel shows the  
10 recovered fluorescence after chymotrypsin activation. For both (A) and (B), Lane 1 =  
11 citrate-capped AuNPs; Lane 2 = peptide substrate, P3; Lane 3 = AuNPs-P3 probe;  
12 Lane 4 = P3 digested by chymotrypsin; and Lane 5 = AuNPs-P3 probe activated by  
13 chymotrypsin. (C) Fluorescence emission spectra of three different AuNPs-peptide  
14 probes activated by chymotrypsin after 1 h incubation.

15  
16 **Figure 3.** Detection characteristics of the AuNPs-P3 probe. (A) Concentration  
17 optimization; and (B) detection specificity to serine proteases, including trypsin (open  
18 diamond) and chymotrypsin (close diamond). Error bars (SD) represent the data from  
19 three independent measurements.

20  
21 **Figure 4.** Chymotrypsin activity assay using the AuNPs-P3 probe. (A) Time course of  
22 chymotrypsin ( $5 \text{ ng mL}^{-1}$ ,  $200 \text{ pM}$ ) treatment. The solid line represents the best fit to  
23 a single exponential function, where  $y = 5699.0523 \cdot (1 - e^{-0.0424x})$  and  $R^2 = 0.995$ ; and  
24 (B) the relationship between chymotrypsin concentration and fluorescence intensity in  
25 a 15 min detection time was determined. The linear correlation from 0.25 to 10 ng

26 mL<sup>-1</sup> of chymotrypsin was confident, for which  $\Delta FL = 506.69$  (chymotrypsin) –  
27 90.82 and  $R^2 = 0.989$ . Error bars (SD) represent the data from three independent  
28 measurements.

29

30 **Figure 5.** Chymotrypsin activity in biological samples from mice sacrificed at 8 h  
31 (C8), 10 h (C10), or 24 h (C24) after the first administration of saline (control) or  
32 cerulein. (A) Plasma amylase, (B) plasma lipase, and (C) pancreatic chymotrypsin.  
33 Error bars (SD) represent data from three independent detections; \* and \*\* indicate  
34 statistical significance at  $p$ -value  $< 0.05$  and  $< 0.01$ , respectively.

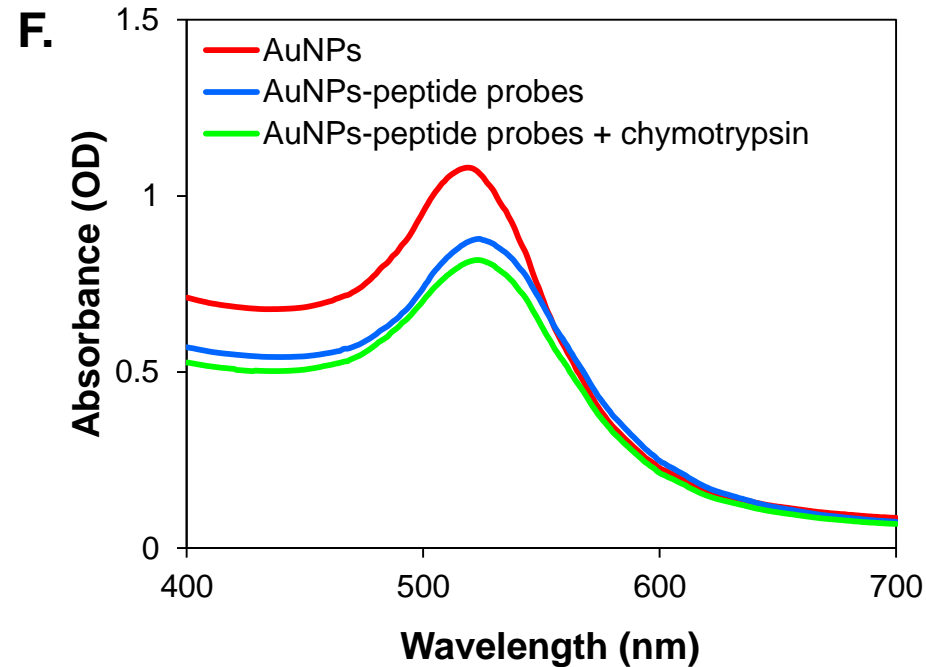
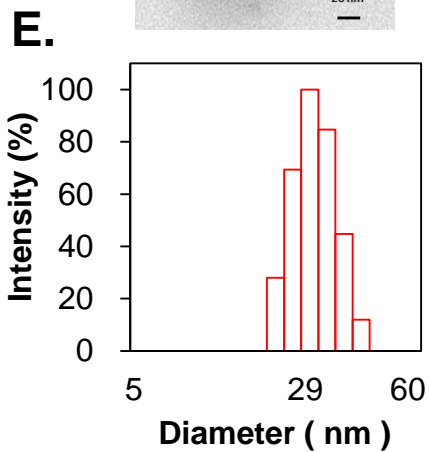
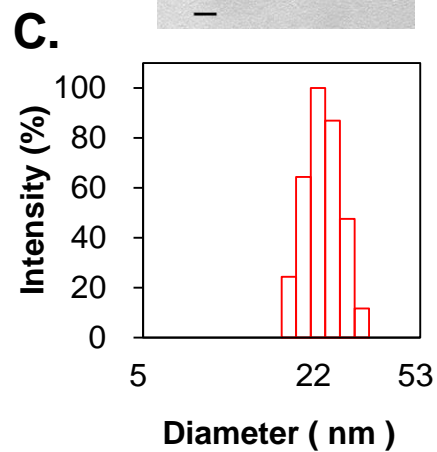
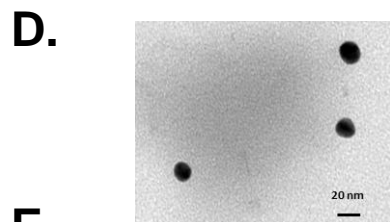
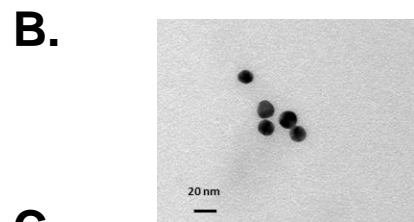
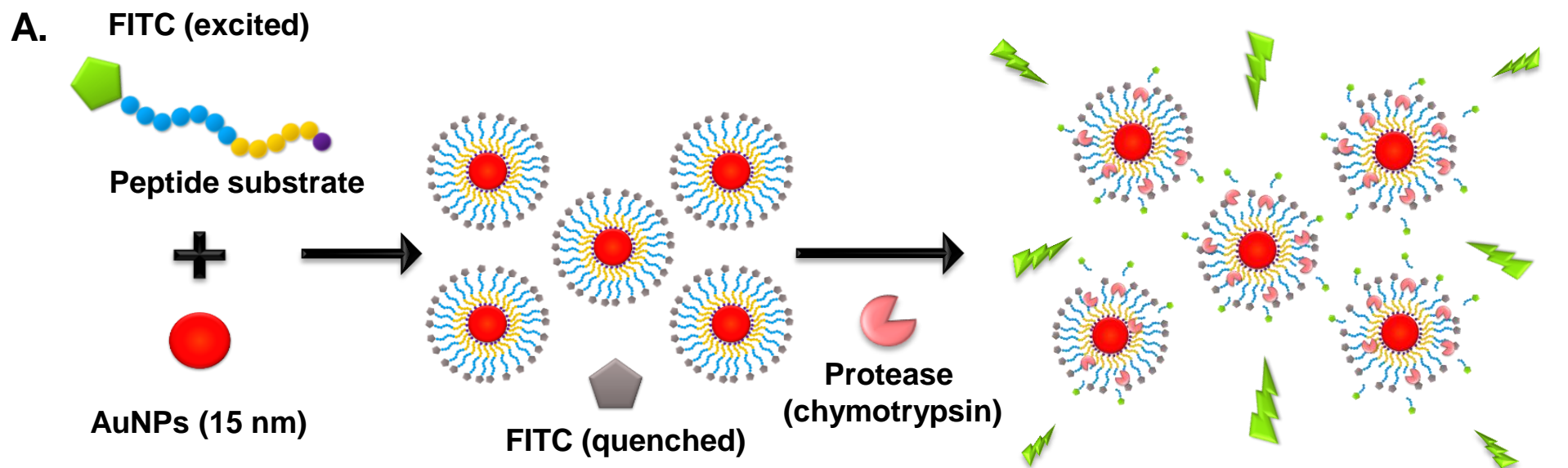
35

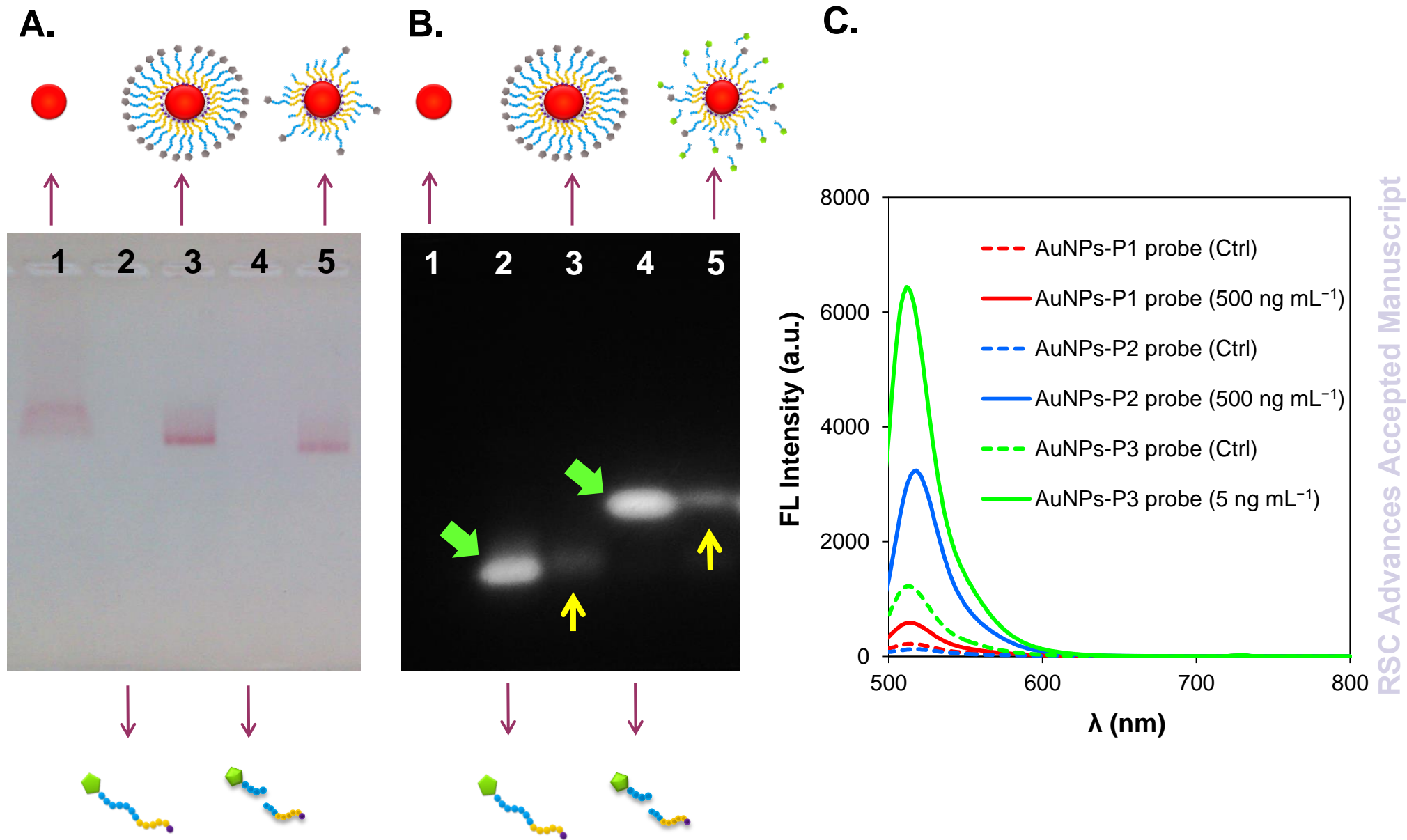
36 **Figure 6.** (A) Duodenal chymotrypsin in mice with cerulein-induced AP; (B) 24 h  
37 time course of fecal chymotrypsin in a cerulein-induced AP mouse model. Every 5 h  
38 period was classified into one group; the grey bar indicates the saline group (control)  
39 and the white bar indicates the cerulein-induced group. Error bars (SD) represent the  
40 data from three independent detections; \* and \*\* indicate statistical significance at  
41  $p$ -value  $< 0.05$  and  $< 0.01$ , respectively.

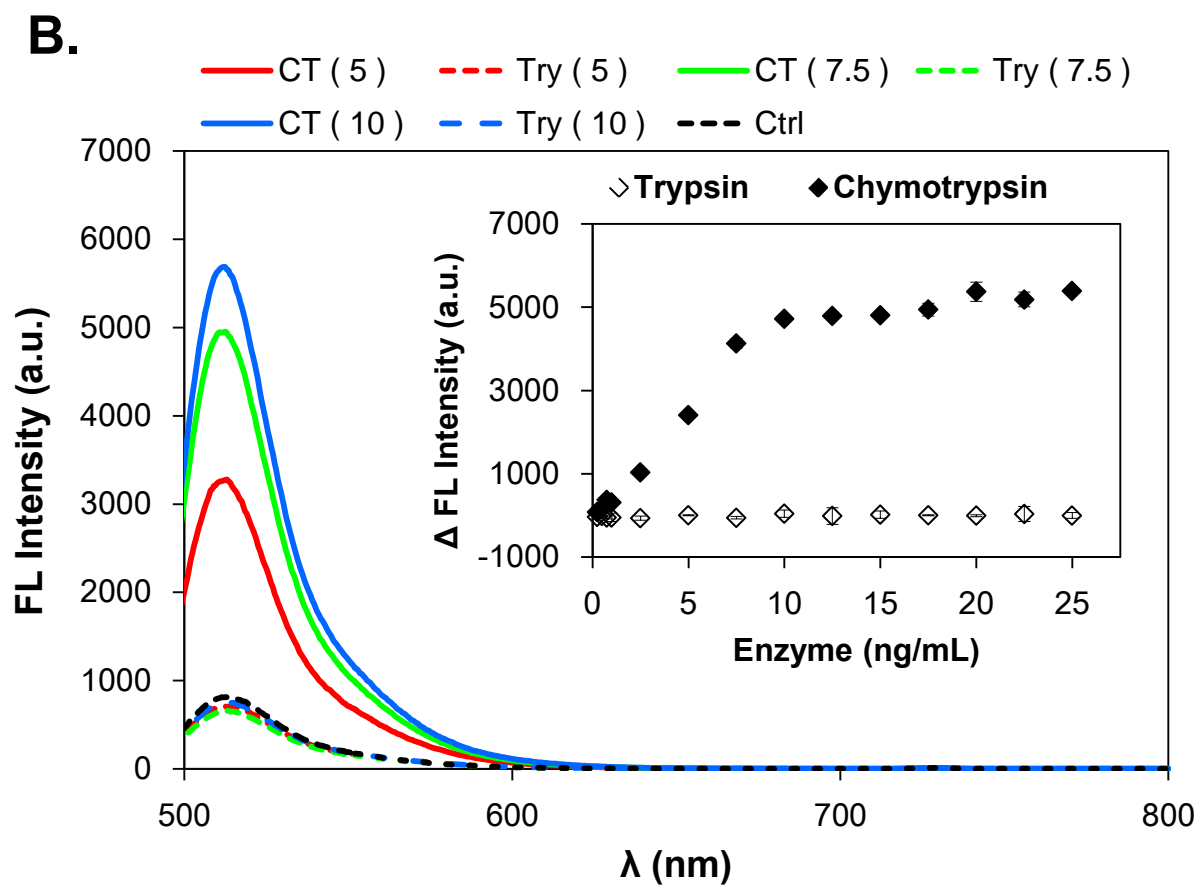
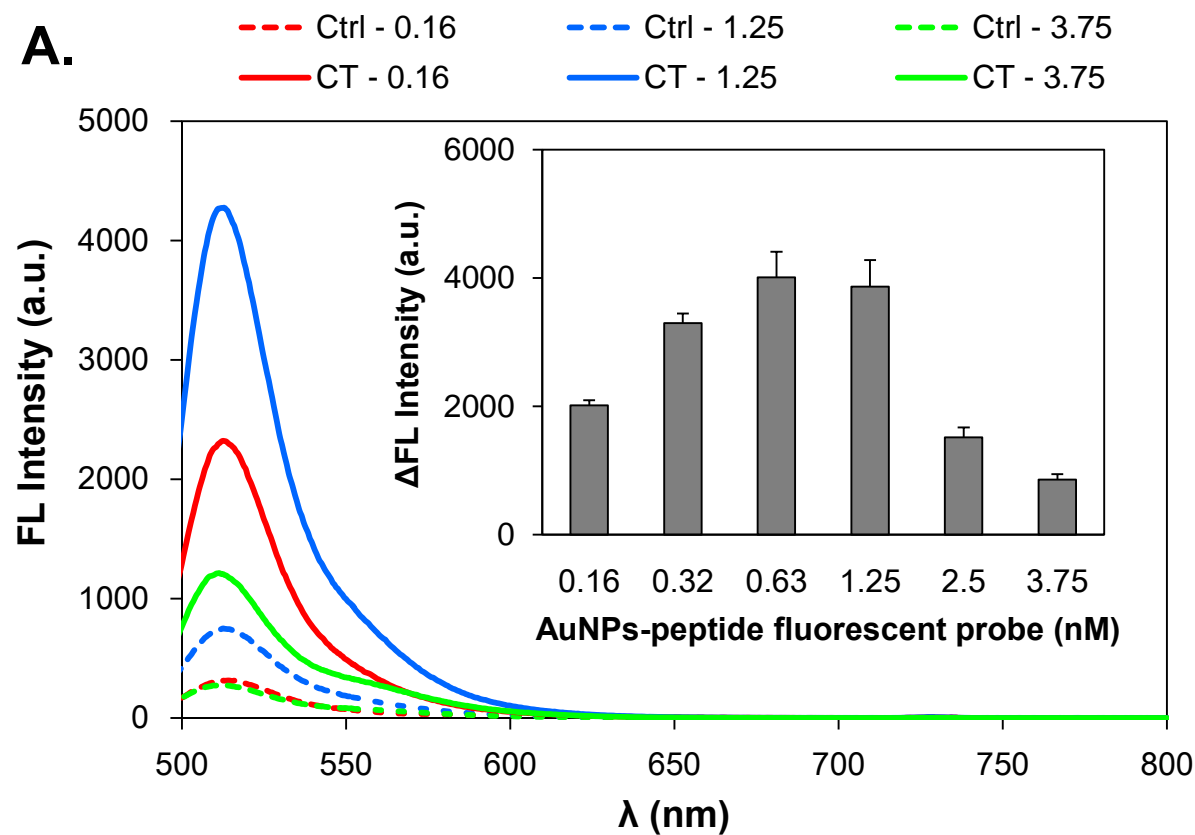
**Table 1.** Peptide sequences corresponding to the chymotrypsin cleavage sites, the pH used during assembly onto the AuNPs, and the optimal detection range and time of the fabricated AuNPs-peptide probes for the assay of chymotrypsin activity.

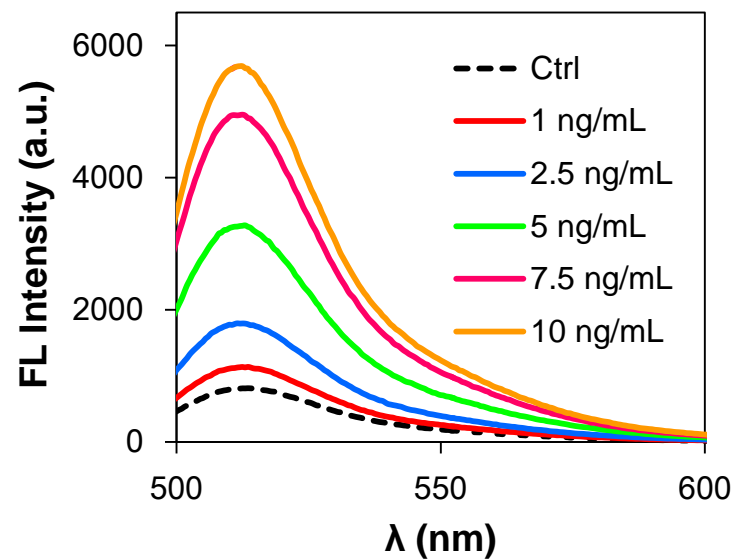
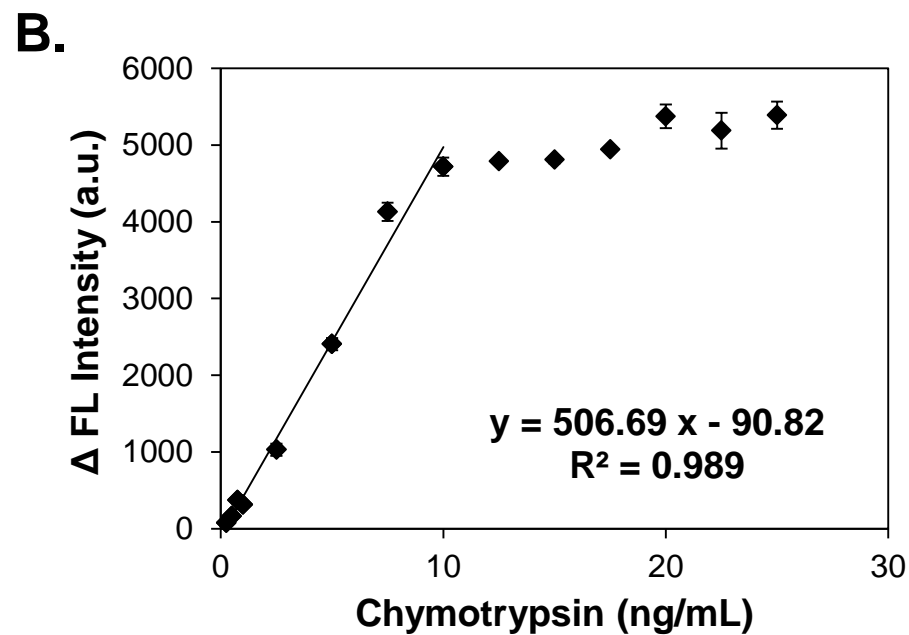
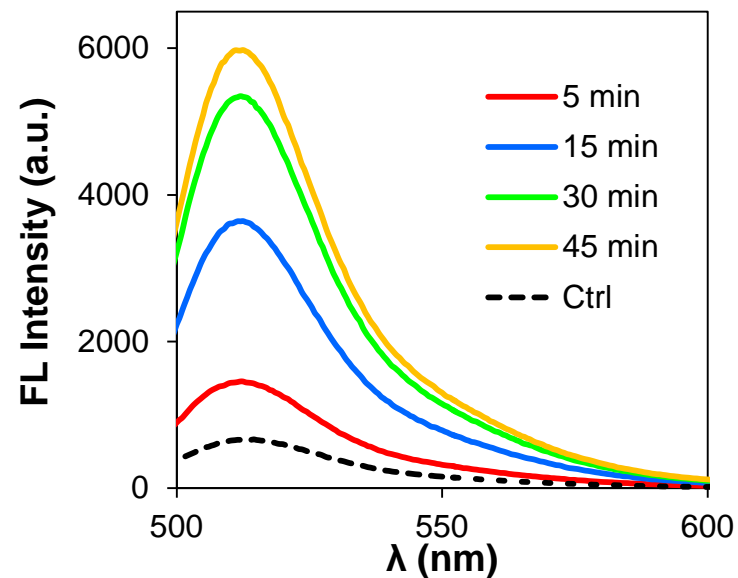
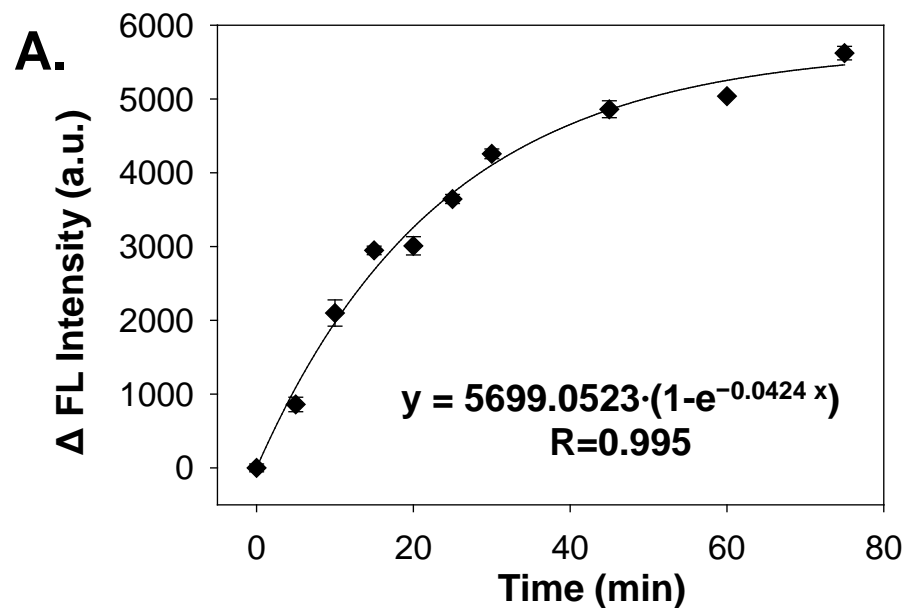
No.	FITC-Acp-peptide	pI	AuNPs fabrication pH	Optimal detection range (ng mL <sup>-1</sup> )	Optimal detection time (min)
<b>P1</b>	GPL ↑ GL ↑ AG(Hyp)C	5.3	7.4	100 – 500	60
<b>P2</b>	GPL ↑ GL ↑ ARGGGGGC	7.8	10.0	25 – 300	30
<b>P3</b>	GPL ↑ GL ↑ ARDDDDDC	3.6	5.6	0.25 – 10	15

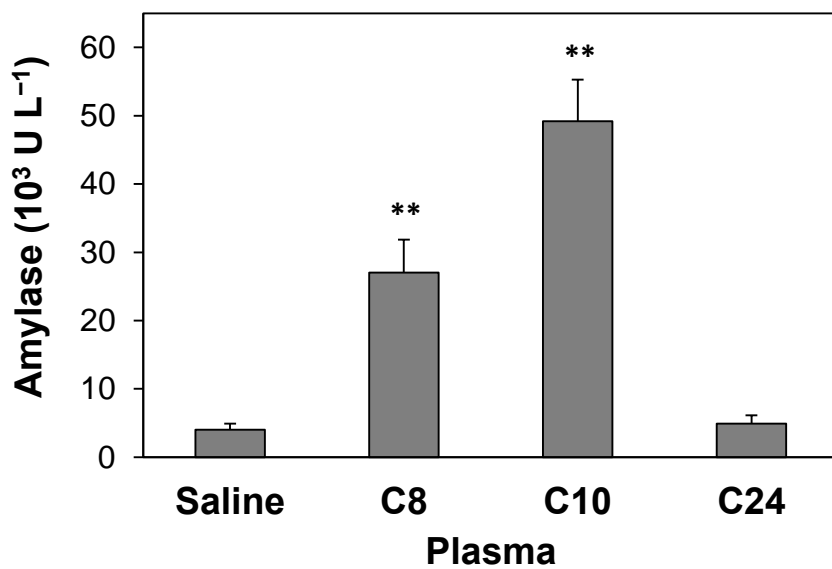
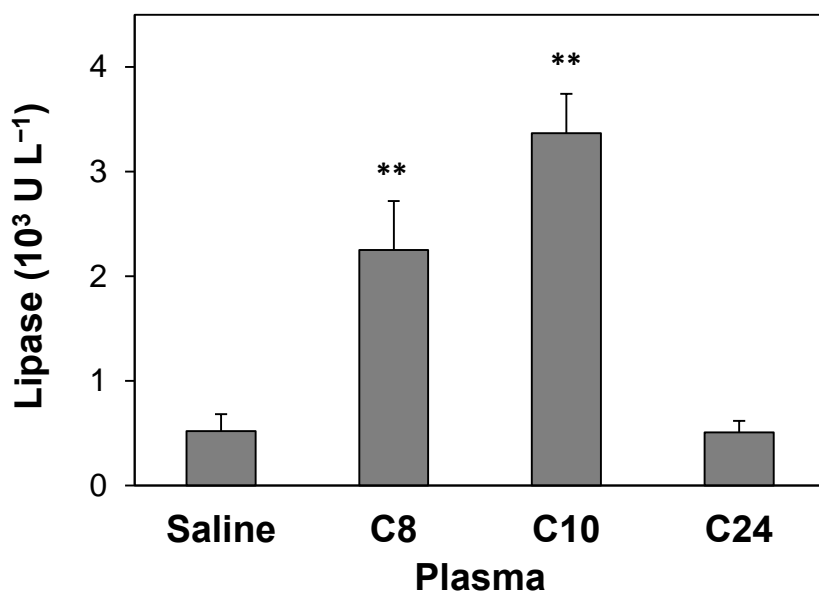
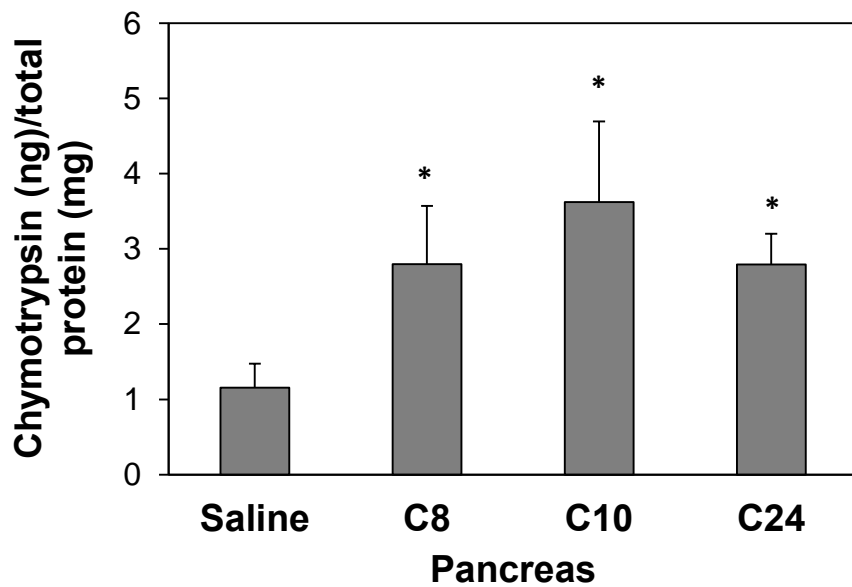
The symbol (↑) indicates the potential cleavage sites cleaved by chymotrypsin. The pI of the peptide substrate was predicted using the online tools — Peptide Property Calculator, Genscript. The optimal detection range of the AuNPs-P1 probe showed a linear correlation of  $\Delta FL = 0.78 (\text{chymotrypsin}) + 7.29$ ,  $R^2 = 0.98$ . The optimal detection range of the AuNPs-P2 probe showed a linear correlation of  $\Delta FL = 4.95 (\text{chymotrypsin}) + 82.35$ ,  $R^2 = 0.99$ . The optimal detection range of the AuNPs-P3 probe showed a linear correlation of  $\Delta FL = 506.69 (\text{chymotrypsin}) + 90.82$ ,  $R^2 = 0.99$ .



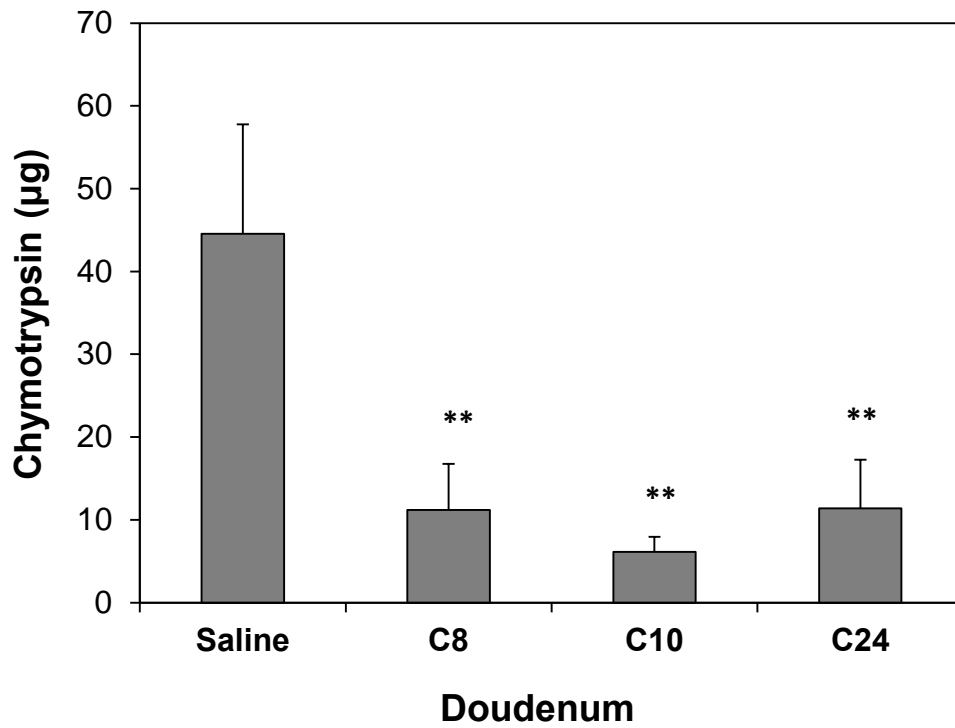






**A.****B.****C.**

A.



B.

